

## Pigments of Life

## Tetrapyrrolic Pigments from Heme- and Chlorophyll Breakdown are Actin-Targeting Compounds

Cornelia A. Karg, Shuaijun Wang, Nader Al Danaf, Ryan P. Pemberton, Denzil Bernard, Maibritt Kretschmer, Sabine Schneider, Themistoklis Zisis, Angelika M. Vollmar, Don C. Lamb, Stefan Zahler, and Simone Moser\*

**Abstract:** Chlorophyll and heme are among the “pigments of life”, tetrapyrrolic structures, without which life on Earth would not be possible. Their catabolites, the phyllobilins and the bilins, respectively, share not only structural features, but also a similar story: Long considered waste products of detoxification processes, important bioactivities for both classes have now been demonstrated. For phyllobilins, however, research on physiological roles is sparse. Here, we introduce actin, the major component of the cytoskeleton, as the first discovered target of phyllobilins and as a novel target of bilins. We demonstrate the inhibition of actin dynamics *in vitro* and effects on actin and related processes in cancer cells. A direct interaction with G-actin is shown by *in silico* studies and confirmed by affinity chromatography. Our findings open a new chapter in bioactivities of tetrapyrroles—especially phyllobilins—for which they form the basis for broad implications in plant science, ecology, and physiology.

## Introduction

Tetrapyrrolic pigments are among the most important natural products on Earth. Some of these pigments are part of

How to cite: *Angew. Chem. Int. Ed.* **2021**, *60*, 22578–22584  
International Edition: doi.org/10.1002/anie.202107813  
German Edition: doi.org/10.1002/ange.202107813

essential processes in living organisms, which brought them the name “pigments of life”.<sup>[1]</sup> Among those, the green pigment chlorophyll (Chl) and the red blood pigment heme play important roles in several biological processes.<sup>[2]</sup> When released from their binding proteins, both substances are toxic and need to be degraded.<sup>[3]</sup> The resulting degradation products are the bilins from the breakdown of heme and the phyllobilins, formed during Chl catabolism.

Bilins are primarily known as the metabolic products of heme catabolism in mammals, but can also be found in lower vertebrates, plants, algae, and bacteria. During heme degradation, heme oxygenase catalyzes the oxygenolytic opening of the macrocycle at one of the four methene bridges furnishing the linear tetrapyrrole biliverdin (BV) (Scheme 1). In the mammalian liver, BV is reduced to bilirubin (BR) by biliverdin reductase A. Originally, bilins were assumed to be waste products of a catabolic pathway, however, extensive literature reports beneficial activities of BR and BV, for example, their potential as strong endogenous antioxidants.<sup>[4]</sup> Moreover, studies demonstrated protective capabilities against a variety of pathological conditions including cardiac injuries, gastrointestinal inflammations, or neurodegenerative diseases.<sup>[5]</sup>

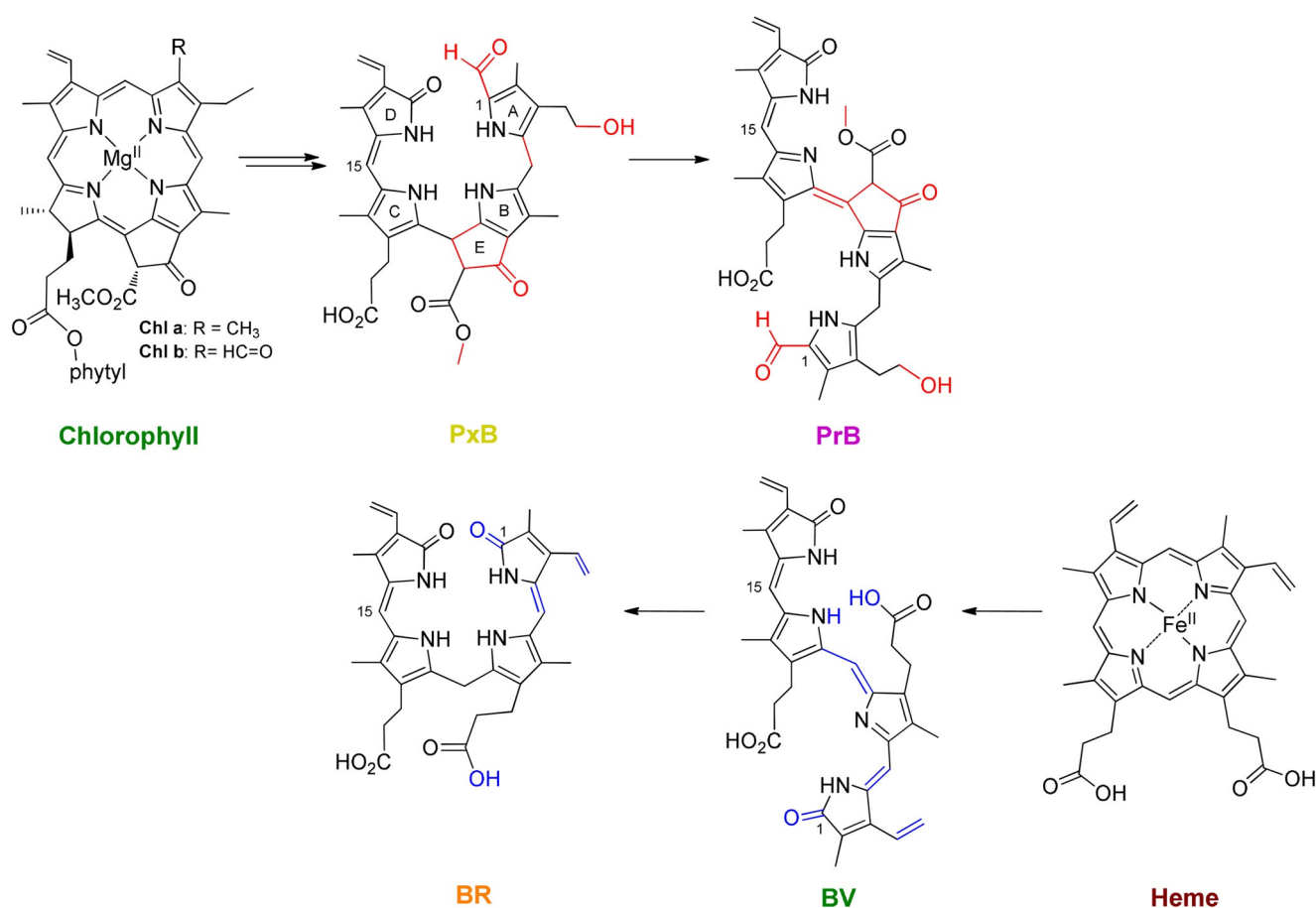
Phyllobilins (PBs) are the degradation products of the green plant pigment Chl and are generated in senescent leaves during autumn as well as in ripening fruit and vegetables.<sup>[6]</sup> PBs were first suspected to be “only” products of a detoxification process, similar to the bilins. The corresponding breakdown process turned out to be much more complex than the degradation of its structural analogue heme, but similarly involving an enzymatic opening of the macrocycle; in the case of Chl degradation catalyzed by pheophorbide a oxygenase.<sup>[7]</sup> In a strictly controlled process, non-colored chlorophyll catabolites, the phylloleucobilins (PleBs), are generated and accumulate in the vacuoles of the plant cell.<sup>[6,8]</sup> In 2008 and 2011, oxidation products of a PleB, so called phylochromobilins, could be identified: a yellow phylloxanthobilin (PxB) and a pink phylloseobilin (PrB).<sup>[9]</sup> In contrast to the enzymatic reduction of BV, the mechanism of the formation of PxB and PrB in plants is not yet elucidated; recent studies, however, suggest an enzymatic “oxidative activity” that effectively transforms PleBs to PxBs.<sup>[10]</sup>

The late stage chlorophyll catabolites PxB and PrB share a remarkable structural similarity with BR and BV.<sup>[6]</sup> PxB resembles the final heme degradation product BR featuring a double bond at C15, whereas PrB, the oxidation product of

[\*] C. A. Karg, Dr. S. Wang, M. Kretschmer, Dr. T. Zisis, Prof. Dr. A. M. Vollmar, Prof. Dr. S. Zahler, Dr. S. Moser  
Pharmaceutical Biology, Department of Pharmacy, Ludwig-Maximilians University of Munich  
Butenandtstraße 5–13, 81377 Munich (Germany)  
E-mail: simone.moser@cup.uni-muenchen.de  
N. Al Danaf, Prof. Dr. D. C. Lamb  
Center for Nanoscience (CeNS) and Nanosystems Initiative Munich (NIM), Department of Chemistry, Ludwig-Maximilians University of Munich  
Butenandtstraße 5–13, 81377 Munich (Germany)  
Dr. R. P. Pemberton, Dr. D. Bernard  
Atomwise Inc.  
717 Market Street, Suite 800, San Francisco, CA 94103 (USA)  
Dr. S. Schneider  
Department of Chemistry, Ludwig-Maximilians University Munich  
Butenandtstrasse 5–13, 81377 Munich (Germany)

Supporting information and the ORCID identification number(s) for the author(s) of this article can be found under:  
<https://doi.org/10.1002/anie.202107813>.

© 2021 The Authors. Angewandte Chemie International Edition published by Wiley-VCH GmbH. This is an open access article under the terms of the Creative Commons Attribution Non-Commercial NoDerivs License, which permits use and distribution in any medium, provided the original work is properly cited, the use is non-commercial and no modifications or adaptations are made.



**Scheme 1.** Structural outline for comparison of heme degradation resulting in bilins, bilirubin (BR) and biliverdin (BV), and late steps of chlorophyll catabolism revealing colored phyllobilins, phylloxanthobilin (PxB, the most commonly identified modification motif is shown<sup>[11]</sup>) and phylloroseobilin (PrB). Structural differences between metabolites of heme and Chl catabolism are highlighted in color.

PxB, represents the analogue of BV due to an extended conjugated  $\pi$ -system. Structural differences become evident in the 1-formyl moiety at ring A and the additional ring E section of the PBs (Scheme 1).

PBs were found to possess very interesting chemical properties and possible bioactivities have already been suggested.<sup>[6,12]</sup> First indications were provided by Müller et al. in 2007, demonstrating that a PleB in peels of apples and pears possesses strong antioxidative activities.<sup>[13]</sup> In the meanwhile, antioxidative properties as well as anti-inflammatory activities could be revealed also for PxBs.<sup>[14]</sup> Furthermore, PxBs were shown to be taken up by cells and to possess promising anti-cancer activities.<sup>[11,15]</sup> In comparison to the bilins, however, investigations on the physiological roles of PBs still lag behind.

Bilins and PBs are ubiquitous tetrapyrrolic structures and the relevance of identifying their targets has become more evident by recent research.<sup>[16]</sup> In general, identification of direct protein interactions is crucial for elucidating detailed mechanisms and mode of action(s) of natural products. Currently, relevant targets for both classes of tetrapyrroles are sparse. In the case of PBs, no human target has yet been identified.

In a functional screening of effects of PBs on cancer cells, we observed inhibition of cell migration by the colored pigments PxB and PrB. Testing their heme-derived counterparts BR and BV for comparison, effects on cell motility were observed as well for the bile pigments. Since the cytoskeletal protein actin plays an essential role in cell motility, control of cell shape, cell division, and intracellular transport,<sup>[17]</sup> we performed imaging experiments using actin staining, which revealed phenotypic changes to the actin cytoskeleton upon treatment with the tetrapyrroles. Cellular processes involving the actin cytoskeleton largely depend on the dynamics of actin filaments, i.e., polymerization and depolymerization.

We demonstrate here that PxB and PrB as well as the bilins BR and BV possess inhibitory effects on *in vitro* actin dynamics and actin-dependent functions in cells. Furthermore, *in silico* docking studies of all four compounds show the potential for direct binding to G-actin, which was supported by affinity chromatography and biophysical approaches.

## Results and Discussion

In the present study, we tested two late stage phyllobilins, a PxB and a PrB (Scheme 1), which were prepared by partial

synthesis as described in the Supporting Information.<sup>[9b,18]</sup> Identities were confirmed by HPLC, UV/Vis, HR-MS, and <sup>1</sup>H-NMR (Figure S1). We aimed to compare these two PBs with their structural counterparts from heme degradation, BR and BV, which are commercially available. We examined the influence of the tetrapyrroles on cell migration using a scratch wound-healing assay in two different human cancer cell lines, T24 and HeLa cells. The scratch assay revealed all tested tetrapyrroles to affect cell migration to a different extent without altering cell viability at concentrations used for the cell migration assay (Figure 1, Figure S2, S3). The PrB appeared to be the most potent compound, which significantly inhibited cell migration even at low nanomolar doses. BR and BV affected cell migration only at high micromolar doses; both showed a significant effect at 100  $\mu$ M in T24 cells.

The actin cytoskeleton is a key player in many cellular processes including cell migration.<sup>[19]</sup> Therefore, we investigated the effects of the four anti-migratory compounds on the actin cytoskeleton in cells. T24 and HeLa cells were treated with PxB, PrB, BR, and BV for 4 hours before the cells were fixed and F-actin stained by a phalloidin rhodamine dye. In cells treated with low micromolar concentrations of PxB and low nanomolar concentrations of PrB, actin agglomerated close to the nucleus, and, in comparison to the control, actin filaments were clearly disorganized (Figure 2). In contrast, incubating cells with BV and BR in concentrations up to 100  $\mu$ M revealed no effect on the organization of actin filaments (Figure S4).

Having established that the tested compounds had an effect on actin and actin-dependent processes in cells, their influence on assembly and disassembly of actin was investigated by different *in vitro* approaches. Using pyrene labeled actin, we assessed the polymerization and depolymerization processes by monitoring the change in pyrene fluorescence intensities upon addition of PxB, PrB, BR, and BV. All four compounds showed an inhibition of actin polymerization compared to the vehicle control. A decelerated polymerization process and a lower plateau of fluorescence intensity was observed in response to PBs and bilins (Figure 3A). Again, PBs were active at lower concentrations than bilins, with PrB affecting polymerization *in vitro* in the low micromolar range.

Furthermore, we investigated the influence of the tetrapyrroles on F-actin depolymerization. All four tetrapyrroles showed an increased depolymerization rate compared to the control sample. Comparing the effects with the actin depolymerizer latrunculin B (LatB)<sup>[20]</sup> measured at 10  $\mu$ M, PrB (measured at 50  $\mu$ M), and PxB and BV (measured at 100  $\mu$ M) all showed enhanced depolymerization rates. BR showed only a slight effect on the rate of depolymerization at a high concentration of 1000  $\mu$ M (Figure 3B).

Using TIRF microscopy, we additionally investigated the effects of the linear tetrapyrroles on actin nucleation, the initial step of the actin polymerization process.<sup>[21]</sup> Nucleation was found to be significantly inhibited by both, PBs and bilins (Figure 3C).

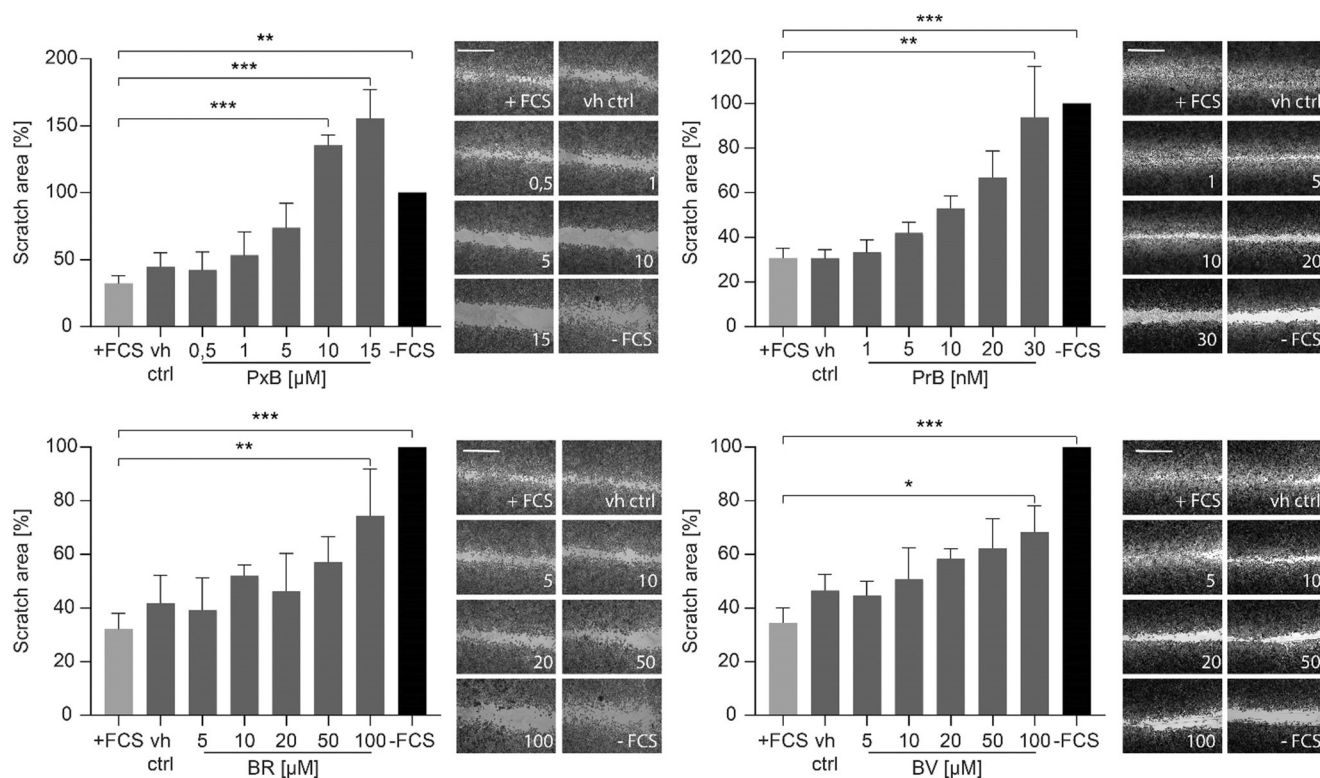


**Figure 1.** Effects of PBs and bilins on cell migration. T24 cells treated with PxB, PrB, BR, BV, and vehicle control (vh ctrl) were analyzed with a scratch wound-healing assay. Treatment with cell medium with FCS served as a negative control and medium without FCS as a positive control. The bar plots indicate the relative scratch gap normalized to the control without FCS given as mean  $\pm$  SEM of three independent experiments performed in triplicates (one-way ANOVA followed by Dunnett's multiple comparison test, \* $P < 0.05$ , \*\* $P < 0.01$ , \*\*\* $P < 0.001$ ). Representative images from the wound healing assay collected 16–24 h after generating the scratch are shown. Scale bar: 1 mm.

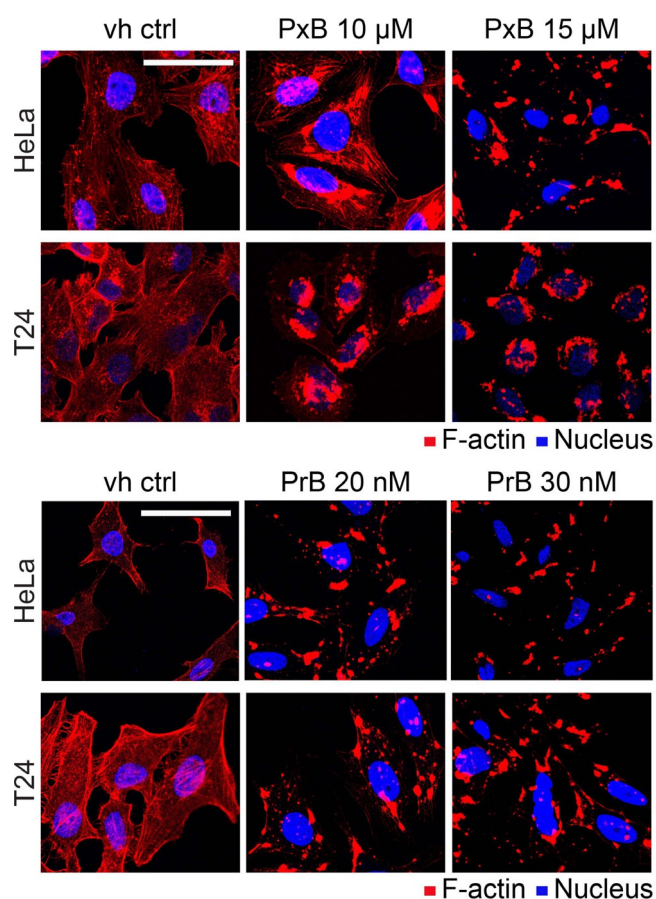


**Figure 2.** Effects of PBs and bilins on F-actin morphology. Images of immunofluorescence stained HeLa and T24 cells treated with PxB and PrB for 4 h. Nuclei were stained with Hoechst (shown in blue) and F-actin with rhodamine-phalloidin (shown in red). Scale bar: 50  $\mu\text{m}$ . Representative images taken from three independent experiments are shown.

In order to investigate whether the observed effects are caused by a direct interaction with G-actin, we used affinity chromatography with G-actin immobilized on sepharose beads. The amount of compounds bound to G-actin beads was analyzed by analytical HPLC and compared with agarose beads, which were used as a negative control for non-specific binding to beads. Upon elution, a significantly higher amount of all compounds released from G-actin beads was observed in contrast to agarose beads (Figure 4A).

Next, we used *in silico* studies to investigate the potential interaction of the tetrapyrroles with G-actin. Docking of the compounds to the binding site of kabiramide C (KabC), a known actin binder,<sup>[22]</sup> indicated several different binding orientations for each molecule. Interestingly, among the different conformations generated for each ligand, a common binding mode shared by all four compounds placed a pyrrolin-2-one ring into a hydrophobic pocket present in G-actin (Figure 4B, C) lined with residues Y133, I136, V139, Y169, and F375 (Figure S5). Upon polymerization of G-actin, this binding site is normally occupied by the D-loop of the next actin monomer in the actin filament and is generally targeted by natural products such as macrolides that promote actin depolymerization.<sup>[23]</sup> The N-vinylformamide moiety in the

critical tail region of KabC also interacts with the same hydrophobic pocket and the lack of specific hydrogen bonds or polar interactions permits the placement of both 17-methyl-18-vinyl-17-pyrrolin-19-one (ring D) as well as 2-methyl-3-vinyl-2-pyrrolin-1-one (ring A) (BR and BV) in the same pocket (for numbering, see Scheme 1). Due to the presence of a number of polar atoms on these compounds, further refinement of docked models should consider both intramolecular and solvent interactions. Confirmation of the predicted binding site was carried out by a competitive pull-down approach using G-actin beads and the actin binding protein profilin, which is known to interact with the common binding site of actin binding proteins and small molecules such as KabC.<sup>[24]</sup> The amount of profilin bound to G-actin was quantified with and without pre-treatment with the compounds and showed a significant decrease of profilin binding for PxB and PrB compared to the vehicle control. These results indicate that PBs are likely to occupy the same binding pocket of G-actin and therefore prevent profilin binding. In contrast, incubation with bilins resulted in a minor reduction of profilin binding (Figure 4D, Figure S6).

The four tested tetrapyrroles, albeit being structurally related, vary greatly in their physico-chemical properties such as solubility, polarity, and fluorescence behavior. To characterize the binding affinity of each compound to G-actin and to determine the dissociation constants ( $K_d$ ), different biophysical techniques were applied, including fluorescence quenching, microscale thermophoresis (MST), and isothermal titration calorimetry (ITC) (Figure 4E, Figure S7–10). The interaction of PxB with G-actin was studied by MST, which was used to monitor the thermophoretic movement of Atto647 labeled G-actin with increasing concentrations of PxB and revealed a  $K_d$  of 65.2  $\mu\text{M}$  (50.6 to 79.8). The binding strength of PrB was determined by fluorescence titration spectroscopy and measuring the quenching of Atto647 labeled G-actin by adding PrB. A  $K_d$  of 1.9  $\mu\text{M}$  (1.5 to 2.5) was determined. Quenching of Atto647 labeled G-actin was also observed during titration with BR. However, saturation of the quenching could not be achieved due to the low solubility of BR. Therefore, a  $K_d$  value could not be determined, but appears to be in the  $\mu\text{M}$  range. For BV, a  $K_d$  of 80.1  $\mu\text{M}$  (67.2 to 93.0) was obtained using ITC. In summary, PxB, PrB, and BV all exhibited binding affinities to G-actin in the low micromolar range, in accordance with the results from biological assays, with the PrB possessing the strongest interaction with G-actin.

BR has been shown to play important cytoprotective roles at physiological concentrations. However, increased concentrations of albumin-bound or unconjugated BR are known to cause hyperbilirubinemia. Several factors such as concentration, conjugation status, or redox state and target location in cells seem to play important roles.<sup>[25]</sup> Therefore, it is questionable whether the herein reported effects of bilins on actin dynamics and actin functions in this high concentration range are of physiological relevance. For PBs, however, which affect actin and related functions at lower concentrations, we provide the basis for elucidating further effects on cellular functions and the underlying mode of actions in more detail. This is of special interest for PrB, the

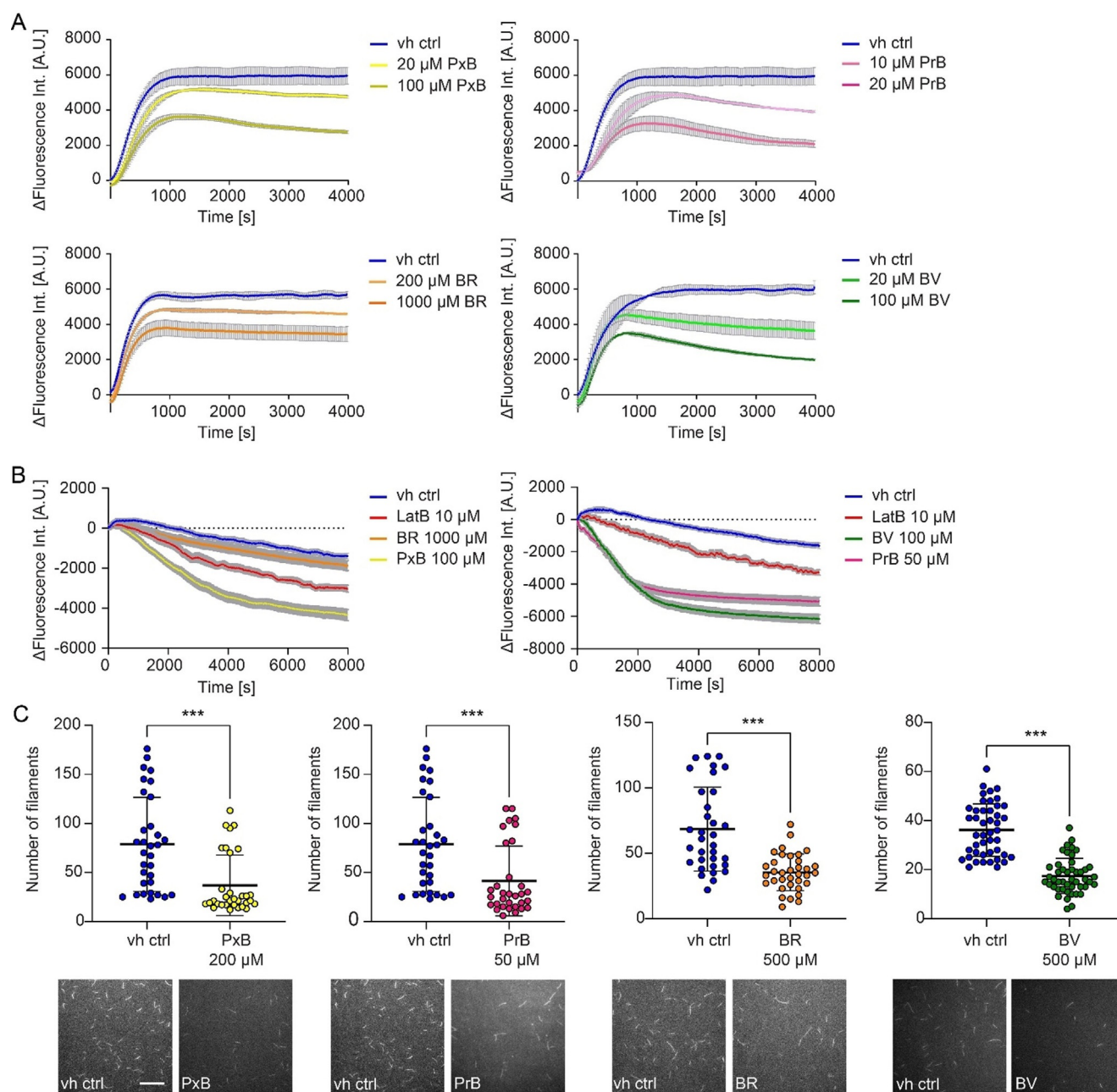


**Figure 3.** Inhibition of in vitro actin dynamics by PBs and bilins. A) Polymerization of pyrene labeled G-actin incubated with PxB, PrB, BR, BV, and a vehicle control (vh ctrl). Data are presented as mean  $\pm$  SEM of three independent experiments performed in duplicates (SEM depicted in grey). B) After allowing the actin to polymerize for 1 h, the depolymerization of pyrene labeled actin was monitored upon addition of PBs, bilins, LatB, and a vehicle control (vh ctrl). Data represent mean  $\pm$  SEM of three independent experiments performed in triplicates (SEM depicted in grey). C) Inhibition of actin nucleation. TIRF assay of Atto488 labeled G-actin incubated with PxB, PrB, BR, BV, and a vehicle control (vh ctrl). The number of actin nuclei present in each frame (calculated from the number of filaments) are presented as a scatter plot. Same controls are shown for PrB and PxB as experiments were performed simultaneously. Average of nuclei  $\pm$  SEM (two-tailed unpaired Student's t-test, \*\*\*  $P < 0.001$ ). Representative images with corresponding vehicle control measurements are shown. Scale bar: 15  $\mu$ m.

most potent candidate, for which no bioactivities have yet been reported. Previous studies have already shown that PxB is a promising anti-cancer reagent, inhibiting the proliferation of cancer cells and inducing apoptosis.<sup>[11]</sup> Furthermore, it was shown that a G2/M-cell cycle arrest is induced at concentrations lower than 20  $\mu$ M. Since the actin cytoskeleton plays an important role in cell division, future studies will investigate the role of actin binding and agglomeration of actin

filaments on the progression of the cell cycle. For both PBs, the identification of actin as a target is an important step towards understanding their bioactivities; the potent inhibition of cancer cell migration at nanomolar concentrations of PrB observed in our study, however, might not solely be due to inhibition of actin polymerization, since the affinity of PrB for actin was observed in the low micromolar range. Hence, it is possible that additional targets for PrB exist.

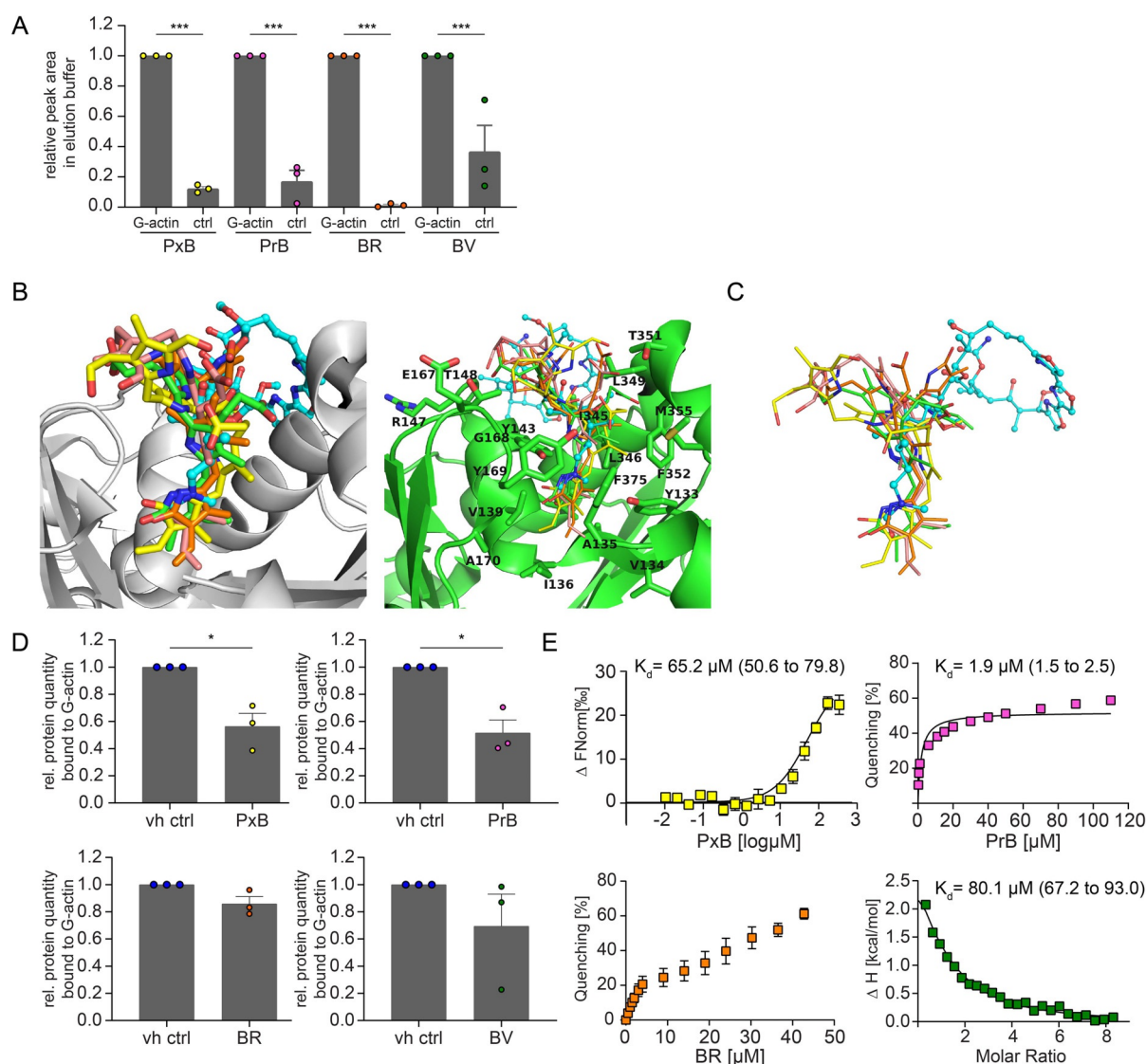


**Figure 4.** Characterization of in vitro binding of PBs and bilins to G-actin. A) G-actin binding assay was performed with G-actin attached to sepharose beads. G-actin or agarose beads (ctrl) were incubated with compounds at 50  $\mu$ M concentration for 1 h before the mixture was centrifuged and washed. Compounds were eluted from beads and the eluate was analyzed by analytical HPLC. Results represent the relative peak area and mean  $\pm$  SEM of three independent experiments (one-way ANOVA followed by Dunnett's multiple comparison test, \*\*\*  $P < 0.001$ ). B) Predicted binding mode of PBs and bilins (carbon atoms shown for PxB in yellow; PrB in pink; BV in green; BR in orange) docked onto actin (grey or green ribbon) (PDB code: 4K41). The residues of actin involved in binding are labeled and shown as sticks. KabC is depicted using a ball and stick model (cyan). C) Overlay of docked conformers of PxB in yellow, PrB in pink, BV in green, BR in orange and KabC in cyan (PDB code: 4K41) showing the pyrrolin-2-one (ring D) occupying the same regions as the N-vinylformamide of KabC. D) Competitive G-actin binding assay of compounds in combination with the actin binding protein profilin. G-actin beads were incubated with PBs or bilins at 50  $\mu$ M concentration for 1 h prior to addition of profilin (0.67  $\mu$ M). Beads were centrifuged and the solubilised pellet fraction was analyzed using SDS-PAGE. The amount of profilin was quantified and normalized to the vehicle control (vh ctrl). Data represent mean  $\pm$  SEM of three independent experiments (two-tailed unpaired Student's t-test with Welch's correction, \*  $P < 0.05$ ). E) Determination of  $K_d$  values using MST for PxB (protein concentration = 71.4 nM), fluorescence quenching for PrB and BR (protein concentration = 200 nM), and ITC for BV (protein concentration = 50  $\mu$ M). A  $K_d$  for BR was not calculated because of the poor fit to the binding model. Results for PxB, PrB, and BR represent mean  $\pm$  SEM of three independent experiments.  $K_d$  values are expressed as mean values (68% CI).

## Conclusion

There are many arguments against the assumption that the breakdown of the “pigments of life” is only a detoxification process. Questions concerning the roles of the degradation products, however, still remain puzzling. Many organisms such as bacteria, plants, or animals produce natural substan-

ces with actin-binding properties<sup>[26]</sup> and accumulating research suggests that these substances play possible roles in host-defense mechanisms.<sup>[27]</sup> Interestingly, PBs were recently associated with plant defense against pathogen attack.<sup>[28]</sup>

PBs and bilins are a class of ubiquitous natural products; both have previously been shown to possess multiple physiologically relevant properties. In this study, by introducing

actin as human target for PBs and for bilins, we go one step further in unravelling the question behind the degradation of two of the most important pigments on Earth. Considering that an estimated  $10^9$  tons of chlorophyll are degraded every year on Earth,<sup>[29]</sup> understanding the effects of the therefore abundant metabolites that are formed during this process, the PBs, opens the door for future studies on the physiological roles of this ubiquitous class of tetrapyrroles.

### Acknowledgements

We would like to thank Kerstin Schmid and Rita Socher for technical support, and Dr. Lars Allmendinger for NMR measurements. We thank Prof. Dr. Michaela Smolle at the Biophysics Core Facility at the Biomedical Center LMU Munich and Dr. Sophie Brameyer at the Bioanalytics Core Facility at the LMU Biocenter for support with ITC and MST experiments. Funding by the Deutsche Forschungsgemeinschaft (DFG, German Research Foundation) is gratefully acknowledged (Prof. Dr. Stefan Zahler and Prof. Dr. Don C. Lamb Project-ID 201269156—SFB 1032 Project B03 and B08, and Dr. Simone Moser Project-ID 448289381). Open access funding enabled and organized by Projekt DEAL.

### Conflict of Interest

The authors declare no conflict of interest.

**Keywords:** actin cytoskeleton · bilins · natural products · phyllobilins · porphyrinoids

- [1] A. R. Battersby, *Nat. Prod. Rep.* **2000**, *17*, 507–526.
- [2] S. Granick in *Evolving Genes and Proteins* (Eds.: V. Bryson, H. J. Vogel), Academic Press, New York, **1965**, pp. 67–88.
- [3] a) K. Apel, H. Hirt, *Annu. Rev. Plant Biol.* **2004**, *55*, 373–399; b) S. Kumar, U. Bandyopadhyay, *Toxicol. Lett.* **2005**, *157*, 175–188.
- [4] R. Stocker, *Antioxid. Redox Signal.* **2004**, *6*, 841–849.
- [5] a) F. H. Bach, *FASEB J.* **2005**, *19*, 1216–1219; b) S. Gazzin, L. Vitek, J. Watchko, S. M. Shapiro, C. Tiribelli, *Trends Mol. Med.* **2016**, *22*, 758–768.
- [6] B. Kräutler, *Angew. Chem. Int. Ed.* **2016**, *55*, 4882–4907; *Angew. Chem.* **2016**, *128*, 4964–4990.
- [7] S. Hörtensteiner, F. Vicentini, P. Matile, *New Phytol.* **1995**, *129*, 237–246.
- [8] S. Hörtensteiner, M. Hauenstein, B. Kräutler in *Advances in Botanical Research*, Vol. 90 (Ed.: B. Grimm), Academic Press, **2019**, pp. 213–271.
- [9] a) M. Ulrich, S. Moser, T. Müller, B. Kräutler, *Chem. Eur. J.* **2011**, *17*, 2330–2334; b) S. Moser, M. Ulrich, T. Müller, B. Kräutler, *Photochem. Photobiol. Sci.* **2008**, *7*, 1577–1581.
- [10] C. Vergeiner, M. Ulrich, C. Li, X. Liu, T. Müller, B. Kräutler, *Chem. Eur. J.* **2015**, *21*, 136–149.
- [11] C. A. Karg, P. Wang, F. Kluibenschedl, T. Müller, L. Allmendinger, A. M. Vollmar, S. Moser, *Eur. J. Org. Chem.* **2020**, 4499–4509.
- [12] a) S. Banala, S. Moser, T. Müller, C. Kreutz, A. Holzinger, C. Lütz, B. Kräutler, *Angew. Chem. Int. Ed.* **2010**, *49*, 5174–5177; *Angew. Chem.* **2010**, *122*, 5300–5304; b) I. Süssenbacher, S. Hörtensteiner, B. Kräutler, *Angew. Chem. Int. Ed.* **2015**, *54*, 13777–13781; *Angew. Chem.* **2015**, *127*, 13981–13985.
- [13] T. Müller, M. Ulrich, K. H. Ongania, B. Kräutler, *Angew. Chem. Int. Ed.* **2007**, *46*, 8699–8702; *Angew. Chem.* **2007**, *119*, 8854–8857.
- [14] a) C. A. Karg, C. Doppler, C. Schilling, F. Jakobs, M. C. S. Dal Colle, N. Frey, D. Bernhard, A. M. Vollmar, S. Moser, *Food Chem.* **2021**, *359*, 129906; b) C. A. Karg, C. M. Schilling, L. Allmendinger, S. Moser, *J. Porphyrins Phthalocyanines* **2019**, *23*, 881–888; c) C. A. Karg, P. Wang, A. M. Vollmar, S. Moser, *Phytomedicine* **2019**, *60*, 152969.
- [15] P. Wang, C. A. Karg, N. Frey, J. Frädrieh, A. M. Vollmar, S. Moser, *Arch. Pharm.* **2021**, e2100061.
- [16] A. Rosa, V. E. Pye, C. Graham, L. Muir, J. Seow, K. W. Ng, N. J. Cook, C. Rees-Spear, E. Parker, M. S. dos Santos, C. Rosadas, A. Susana, H. Rhys, A. Nans, L. Masino, C. Roustan, E. Christodoulou, R. Ulferts, A. G. Wrobel, C.-E. Short, M. Fertleman, R. W. Sanders, J. Heaney, M. Spyer, S. Kjør, A. Riddell, M. H. Malim, R. Beale, J. I. MacRae, G. P. Taylor, E. Nastouli, M. J. van Gils, P. B. Rosenthal, M. Pizzato, M. O. McClure, R. S. Tedder, G. Kassiotis, L. E. McCoy, K. J. Doores, P. Cherepanov, *Sci. Adv.* **2021**, *7*, 22.
- [17] T. D. Pollard, J. A. Cooper, *Science* **2009**, *326*, 1208–1212.
- [18] C. Li, M. Ulrich, X. Liu, K. Wurst, T. Müller, B. Kräutler, *Chem* **2014**, *5*, 3388–3395.
- [19] X. Trepate, Z. Chen, K. Jacobson, *Comprehensive Physiology*, Vol. 2, Wiley, Hoboken, **2012**, pp. 2369–2392.
- [20] M. May, T. Wang, M. Müller, H. Genth, *Toxins* **2013**, *5*, 106–119.
- [21] R. Dominguez, *Crit. Rev. Biochem. Mol. Biol.* **2009**, *44*, 351–366.
- [22] J. Tanaka, Y. Yan, J. Choi, J. Bai, V. Klenchin, I. Rayment, G. Marriott, *Proc. Natl. Acad. Sci. USA* **2003**, *100*, 13851–13856.
- [23] S. Wang, F. A. Gegenfurtner, A. H. Crevenna, C. Ziegenhain, Z. Kliesmete, W. Enard, R. Müller, A. M. Vollmar, S. Schneider, S. Zahler, *J. Nat. Prod.* **2019**, *82*, 1961–1970.
- [24] R. Dominguez in *Actin-Monomer-Binding Proteins* (Ed.: P. Lappalainen), Springer New York, New York, **2007**, pp. 107–115.
- [25] J. Kapitulnik, *Mol. Pharmacol.* **2004**, *66*, 773–779.
- [26] R. Ueoka, A. R. Uria, S. Reiter, T. Mori, P. Karbaum, E. E. Peters, E. J. N. Helfrich, B. I. Morinaka, M. Gugger, H. Takeyama, S. Matsunaga, J. Piel, *Nat. Chem. Biol.* **2015**, *11*, 705–712.
- [27] G. Lackner, E. E. Peters, E. J. N. Helfrich, J. Piel, *Proc. Natl. Acad. Sci. USA* **2017**, *114*, E347–E356.
- [28] S. Moser, T. Erhart, S. Neuhauser, B. Kräutler, *J. Agric. Food Chem.* **2020**, *68*, 7132–7142.
- [29] G. A. F. Hendry, J. D. Houghton, S. B. Brown, *New Phytol.* **1987**, *107*, 255–302.

Manuscript received: June 11, 2021

Revised manuscript received: July 22, 2021

Accepted manuscript online: July 26, 2021

Version of record online: August 31, 2021